

RSC Advances



This is an *Accepted Manuscript*, which has been through the Royal Society of Chemistry peer review process and has been accepted for publication.

Accepted Manuscripts are published online shortly after acceptance, before technical editing, formatting and proof reading. Using this free service, authors can make their results available to the community, in citable form, before we publish the edited article. This *Accepted Manuscript* will be replaced by the edited, formatted and paginated article as soon as this is available.

You can find more information about *Accepted Manuscripts* in the [Information for Authors](#).

Please note that technical editing may introduce minor changes to the text and/or graphics, which may alter content. The journal's standard [Terms & Conditions](#) and the [Ethical guidelines](#) still apply. In no event shall the Royal Society of Chemistry be held responsible for any errors or omissions in this *Accepted Manuscript* or any consequences arising from the use of any information it contains.

Cite this: DOI: 10.1039/c0xx00000x

www.rsc.org/xxxxxx

Paper

Near Infrared Fluorescent/Ultrasonic Bimodal Contrast Agent for Imaging Guided pDNA Delivery via Ultrasound Targeted Microbubble Destruction

Yongbo Yang,^a Jinrui Wang,^b Xiaoda Li,^a Li Lin,^a Xiuli Yue^{a*}⁵ Received (in XXX, XXX) Xth XXXXXXXXXX 20XX, Accepted Xth XXXXXXXXXX 20XX

DOI: 10.1039/b000000x

This paper reported the development of multifunctional contrast agent for near infrared (NIR) fluorescent/ultrasonic bimodal imaging and gene delivery. CuInS₂-ZnS alloyed quantum dots (ZCIS QDs) were coated with polyethyleneimine (PEI) to complex plasmid DNA (pDNA), followed by adsorption onto the surface of microbubbles (MBs) generated from the surfactant mixture of Span 60 and Tween 80. It was found that the obtained composite agent of MBs@QDs@PEI/pDNA had excellent capability to enhance both ultrasound and fluorescence imaging. In addition, *in vitro* cell experiment showed that pDNA could be released from MBs@QDs@PEI/pDNA and internalized by target HeLa cells to realize a relative high transfection efficiency by ultrasound-targeted microbubble destruction. Furthermore, the cytotoxicity, immune toxicity and histological evaluation showed that MBs@QDs@PEI/pDNA had a good biocompatibility for medical application. Therefore, such a multifunction agent could operate as a promising platform for targeting gene delivery under the guidance of NIR fluorescent/ultrasonic bimodal imaging.

Introduction

Gene therapy is a promising therapeutic option to treat various kinds of genetic and acquired diseases, which involves the introduction of exogenous gene or nucleotides into host cells.^{1, 2} Due to the instability and low cellular uptake of naked gene, different gene delivery systems (viral and non-viral vectors) have been developed.^{3, 4} However, one of the obstacles for successful gene therapy is the insufficient delivery of genes to target tissues and the incapacity to monitor gene delivery and therapeutic responses at the targeted site.⁵⁻⁹ Exhilaratingly, the emergence of molecular imaging strategies has enabled us to optimize gene therapy by evaluating the effectiveness of gene delivery noninvasively and spatiotemporally. In addition, the unique characteristics of numerous functional nanoparticles make them promising candidates to accomplish gene delivery with the necessary feature of visualizing the delivery.

Imaging with contrast agent allows noninvasive diagnosis of the disease and real-time monitoring of the particle localization. However, the traditional non-viral vectors such as cationic liposomes and polymer nanoparticles show limitations in monitoring the DNA delivery process.^{10, 11} Quantum dots (QDs) have been used as non-viral vectors and make gene therapy to be observed through fluorescence imaging.¹²⁻¹⁶ In recent years, the heavy metal-free ZnCuInS or CuInS₂-ZnS alloyed (ZCIS) QDs have been reported to exhibit highly efficient and widely tunable fluorescence from the visible to near infrared (NIR) region by varying not only the size but also the composition of particles,^{17,}

¹⁸ allowing higher tissue penetration than visible optical probes for *in vivo* imaging applications at the NIR window of 650–900 nm,¹⁹ and longer fluorescent time than organic dye.²⁰⁻²² Compared with most of the highly luminescent QDs, such as CdTe, CdSe and PbS,²³⁻²⁵ ZCIS QDs contain no toxic element, showing great potential in biomedical applications.

Ultrasound imaging is the most widely used imaging modality due to its features of real-time, low cost and high safety. With the use of ultrasound contrast agents, such as gas-filled microbubbles (MBs), the resolution and sensitivity of clinical ultrasound imaging have made great improvements.²⁶⁻²⁸ Recently, gas-filled MBs have been developed as efficient controlled-release carriers for targeted gene or drug delivery through ultrasound-targeted microbubble destruction (UTMD) technique.²⁹⁻³¹ UTMD involves the attachment of genes or drug to gas-filled microbubbles, which are then injected intravenously and destroyed at target tissues by enhanced ultrasound irradiation.³²⁻³⁵ The acoustic power required to induce sonoporation, i.e. generate transient ultrasound-induced perforations in cell membranes, was significantly reduced when MBs were present.³⁶ Microvessel ruptures likely due to cavitation provided focal delivery of colloidal particles and red blood cells in a given tissue.³⁷

This paper reported the fabrication of NIR fluorescent/ultrasonic bimodal contrast agent by layer-by-layer (LbL) self-assembly technique.³⁸ In brief, Plasmid DNA (pDNA) complexed ZCIS QDs were adsorbed onto the surface of ST68 MBs for imaging guided pDNA delivery (Figure 1). ZCIS QDs were coated with polyethyleneimine (PEI) to complex pDNA. Through UTMD, the “soft” ST68 MBs could release

QDs@PEI/pDNA, which could penetrate into target tissue to achieve efficient gene therapy under the guidance of NIR

fluorescent/ultrasonic bimodal imaging.

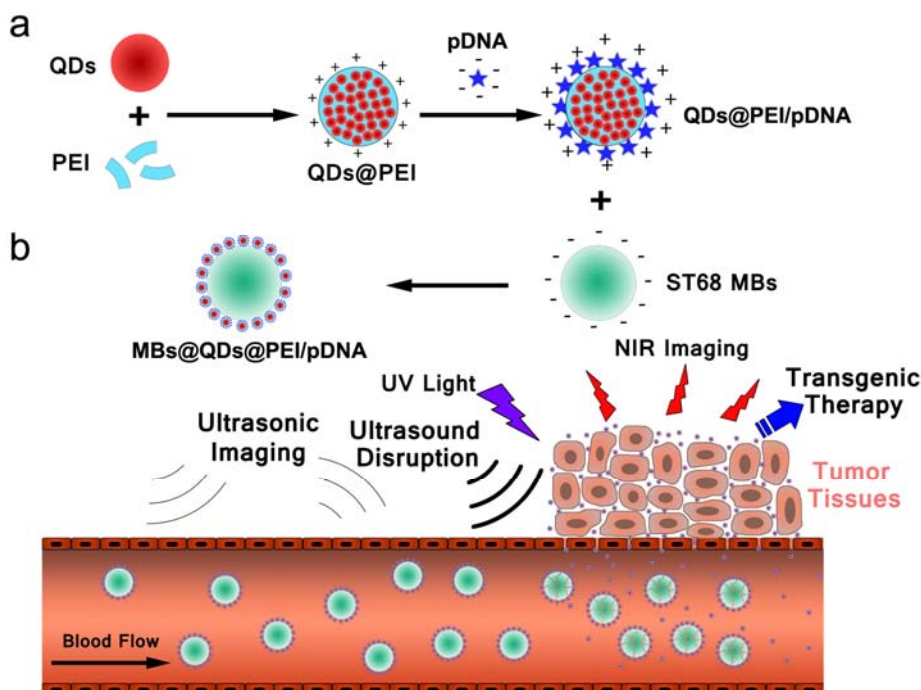


Figure 1. Schematic illustration: (a) Formation of MBs@QDs@PEI/pDNA; (b) NIR fluorescent/ultrasonic bimodal imaging and targeted delivery of pDNA through UTMD.

Materials and Methods

Materials

Copper(I) iodide (CuI, 99.995%) was purchased from J&K. Indium(III) acetate (99.99%) was purchased from Alfa Aesar. 1-dodecanethiol (98%), stearic acid (90%), zinc acetate (99%), octadecylamine (97%) and octadecene (90%) were purchased from Aladdin. Span 60, Tween 80 and PEI were purchased from Sigma. All chemicals were used without further purification.

Synthesis of ZCIS QDs

The ZCIS QDs were prepared using the modified method according to the literature.³⁹ A Zn precursor solution was prepared by dissolving 8 mmol zinc acetate, 6 mL octadecylamine, and 14.0 mL of octadecene in a three-neck flask, followed by heating to 160 °C under N₂ flow. After keeping at this temperature for about 10 min, the obtained clear colorless solution was stored at 50 °C for use. Then, 0.1 mmol indium acetate, 0.1 mmol CuI, 0.3 mmol stearic acid, 1 mL of 1-dodecanethiol, 8 mL of octadecene were loaded into a 50 mL three-necked flask under an N₂ atmosphere. The mixture was heated to 120 °C under magnetic stirring for 30 min, backfilled with N₂, and then heated to 230 °C. As the temperature increased, the color of the reaction solution progressively changed from slight yellow to red, brown, and finally black. After 20 min, a 1.25 mL of Zn precursor solution was injected into the reaction mixture in 5 batches with a time interval of 15 min. Another 15 min later, the reaction mixture was allowed to cool to 60 °C, and 20 mL of toluene was added thereafter. Upon addition of an equal volume of methanol, the solution was centrifuged at 8 000 rpm

for 20 min. The supernatant was discarded and the precipitate was dispersed by toluene. The obtained ZCIS QDs were purified by repeated centrifugation and decantation.

Preparation of ST68 MBs

ST68 MBs were prepared as described previously.⁴⁰ In brief, 1.48 g Span 60, 1.0 mL Tween 80 and 1.50 g NaCl were well mixed and suspended in 50 mL phosphate buffer solution (PBS) (pH=7.4), then probe-sonicated continuously by a 1.27 cm (1/2 inch) diameter titanium alloy horn (Sonicator 4000, Misonix, Farmingdale, NY, USA) with the maximum output amplitude setting under the atmosphere of perfluoropropane (PFP) gas for 3 min. The resulting suspension was allowed to stand for about 60 min to be separated into three layers. ST68 MBs were then collected from the middle layer and washed three times by PBS. Eventually, ST68 MBs were 1:1 (v:v) suspended in PBS, protected by PFP gas, sealed and stored at 4 °C.

Formation QDs@PEI and QDs@PEI/pDNA complexes

1.2 mmol ZCIS QDs toluene solution were added into 20 mL PEI aqueous solution (50 mg mL⁻¹), allowed for probe-sonication for 5 min by a microtip ultrasonic probe with the maximum output amplitude setting. Then, the mixture were stirred intensely to remove the remaining organic solvents. After the mixture became clear, the QDs@PEI complex was purified by centrifugation at 100 000 g for 60 min and washed with deionized water to remove residual PEI. Finally, QDs@PEI was dispersed in deionized water and stored at 4 °C for further use.

The QDs@PEI/pDNA complexes were prepared by adding 1 mL different concentration of QDs@PEI aqueous solution to 1 mL plasmid pDNA (pEGFP-C1) PBS solution (5 µg mL⁻¹) and

vortexed gently. The complexes were incubated at room temperature for 20 min.

Gel Electrophoresis analysis

Agarose gel electrophoresis was used to evaluate the conjugate ability between plasmid pDNA and different concentrations of QDs@PEI. 5 μ L QDs@PEI/pDNA complexes were mixed with 5 μ L $6 \times$ loading buffer, and analyzed on a 0.7 % agarose gel at 110V in $1 \times$ Tris-acetate-EDTA (TAE) buffer for 20 min (PowerPac Universal, Bio-Rad). After electrophoresis, the gel was illuminated with an ultraviolet trans-illuminator (BioSpectrum 410 gel imaging system) for fluorescence imaging of the emission bands.

Adsorption of QDs@PEI/pDNA onto the ST68 MBs surface

0.06 mmol QDs@PEI/pDNA aqueous solution (containing 0.5 mol L^{-1} NaCl) was added into 5 mL ST68 MBs suspension (1×10^7 MBs per 1 mL) in the self-made centrifuge tube (with a drainage port at the bottom). The mixture was slightly shaken for 10 min to allow the sufficient adsorption reaction, then centrifuged by using a bucket-rotor centrifuge (Allegra 6, Beckman Coulter, Fullerton, CA, USA) at 500 g for 5 min. This step made almost all the gas bubbles float to the top, under which the excessive QDs@PEI/pDNA were discarded. The obtained MBs@QDs@PEI/pDNA were then resuspended and washed by 5 mL PBS for three times.

Characterization

UV-vis absorption and fluorescence spectra were obtained on a Cary Eclipse (Varian) 4000 UV-vis spectrophotometer and a Cary Eclipse (Varian) fluorescence spectrophotometer, respectively. All optical measurements were performed at room temperature. The morphology and structure of nanoparticles were test using a transmission electron microscope (TEM, FEI Tecnai G2 Sphera, FEI, Hillsboro, USA). The static light scattering measurements were performed on a particle size distribution analyzer (Horiba LA-920). The surface potentials of MBs and nanoparticles were determined with a PALS/90 Plus Particle Sizing and Potential Analyzer (Brookhaven, Holtsville, NY, USA).

In vitro and in vivo ultrasound imaging

A latex tube simulating as the blood vessel phantom was immersed into a water tank in which an ultrasound probe was pointing closely at the tube. The freshly prepared MBs@QDs@PEI/pDNA was diluted with 0.9 % saline and injected into a latex tube (with an inner diameter of 5 mm) and circulated in the tube by a constant flow pump in a permanent flow rate of 60 mL min^{-1} . Ultrasonograph was performed using a broadband linear array L9-3 transducer (9-3 MHz extended) of the IU22 Ultrasound System (Philips Medical Systems, Solingen, Germany) from the vertical cross-section of the tube. The pulse inversion harmonic imaging (PIHI) mode with a mechanical index (MI) of 0.06 was applied to acquire contrast-enhanced images.

For *in vivo* ultrasound imaging, three New Zealand white rabbits ($n=3$ for each group) were anesthetized with pentobarbital sodium (2.0 mL kg^{-1} weight, 2 % w/v in 0.9 % saline). 0.2 mL of MBs@QDs@PEI/pDNA suspension (300 μ M equivalent

concentration of QDs@PEI in 0.9 % saline) was injected through the ear vein and flushed with 1.0 mL saline. The kidney was imaged transabdominally using a broadband L9-3 transducer in PIHI mode with MI of 0.06. The average grey scale of a selected region of interest (ROI) was analyzed using the IU22 Ultrasound System.

In vivo fluorescence imaging

In vivo fluorescence imaging of MBs@QDs@PEI/pDNA was performed with an small animal imaging system (IVIS Spectrum, Perkin Elmer Life Sciences, Hopkinton, MA, USA) set at excitation 430 nm and emission 700 nm. 200 μ L MBs@QDs@PEI/pDNA (300 μ M equivalent concentration of QDs@PEI in 0.9 % saline) was injected subcutaneously in the back of nude mouse ($n=3$ for each group). The total fluorescence intensity of ROI was analyzed using the small animal imaging system. All the animal experiments were approved by the institutional animal use committee and carried out ethically and humanely.

Cytotoxicity evaluation

Human umbilical vein endothelial (HUVEC) cells and HeLa cells were used to evaluate the cytotoxicity of MBs@QDs@PEI/pDNA through MTT method. HUVEC cells and HeLa cells were seeded in 96-well plate at a density of 5×10^4 cells per well for 24 h respectively. The cells were washed three times with PBS, followed by incubation with 200 μ L different concentration of MBs@QDs@PEI/pDNA, QDs@PEI/pDNA or PEI/pDNA at 37 $^{\circ}C$ and 5 vol.% CO_2 for 48 h. Cell viability was measured using the MTT assay.

Immune toxicity evaluation

Bone marrow dendritic cells (BMDC) were obtained by culturing bone marrow stem cells of SD rat with 20 ng mL^{-1} recombinant granulocyte/macrophage colony stimulating factor in complete Iscove's Modified Dulbecco's Medium (cIMDM) for 6 days at 37 $^{\circ}C$, 5 vol.% CO_2 . Cells were seeded at 5×10^5 cells mL^{-1} in cIMDM for pulsing with MBs@QDs@PEI/pDNA.

We further investigated whether MBs@QDs@PEI/pDNA are able to stimulate T cell proliferation *in vitro*. T cells were obtained from SD rat and cultured in cIMDM at 37 $^{\circ}C$, 5 vol.% CO_2 . Cells were seeded at 5×10^5 cells mL^{-1} in cIMDM for pulsing with MBs@QDs@PEI/pDNA.

Viability of cells after incubating with MBs@QDs@PEI/pDNA for 24 h was determined with by staining with both calcein acetoxymethyl ester (calcein-AM) and propidium iodide (PI) and verified with fluorescence microscopy images. Viable cells can be stained as green fluorescence from calcein-AM, and red fluorescence from PI indicates dead cells. The cell viabilities were also detected by MTT assay.

Histological evaluation

To further investigate the biocompatibility of MBs@QDs@PEI/pDNA, major organs including heart, liver, spleen, lung and kidneys were collected at day 1, day 7 and day 30 after injection of MBs@QDs@PEI/pDNA via the tail vein (200 μ L, 300 μ M per mice), and then fixed in 10% formalin, conducted with paraffin embedded sections, stained with hematoxylin and eosin (H&E), and examined under a digital

microscope. Healthy mice without MBs@QDs@PEI/pDNA injection were used as controls. The body weight of mice were measured every 2 days.

Cellular uptake of QDs@PEI/pDNA

HeLa cells were seeded in 6-well plates and incubated with QDs@PEI/pDNA at the concentration of 300 μM for 24 h at the environment of 37 $^{\circ}\text{C}$ and 5 vol.% CO_2 . Afterwards, the cells were washed with fresh PBS and stained with LysoTracker Green DND (invitrogen L7526) and 4',6-diamidino-2-phenylindole (DAPI) for microscopic observation on a confocal laser scanning microscopy (CLSM) 510 (Carl Zeiss, Oberkochen, Germany) at excitation of 430 nm.

Transfection experiment

HeLa cells were seeded in 24-well plates at a density of 1×10^5 cells per well for 24 h. pEGFP-C1 loaded samples (QDs@PEI/pDNA or MBs@QDs@PEI/pDNA) were diluted to a certain concentration with serum-free medium and added to cell cultures for transfection. Ultrasound irradiation was carried out on an ultrasound transfection instrument (Sonopore KTAC-4000, NepaGene, Chiba, Japan). The 24-well plate was placed above a transducer with a thin layer of ultrasound coupling medium, and only one well of MBs@QDs@PEI/pDNA at a time was exposed to ultrasound for 30 s (0.8 W cm^{-2}). The medium was replaced with serum-containing medium after 4 h transfection. The transfection ability was monitored at 24h, 48h and 72h post-transfection by fluorescence microscopy. Approximately 72 h post-transfection, cells were prepared for quantitative analysis by flow cytometry.

Statistical analysis

Analysis of variance (ANOVA) and *t*-tests were used to analyze the data. The level of significance in statistical analyses was defined as $p < 0.05$.

Results and Discussion

Preparation and Characterization of QDs@PEI, QDs@PEI/pDNA and MBs@QDs@PEI/pDNA

ZCIS QDs were prepared in a noncoordinating solvent octadecene using acetate salts of Cu, In, and Zn as cation precursor in the presence of stearic acid and dodecanethiol according to the reported method.³⁹ PEI, which is amphiphilic and soluble in many polar solvents and sufficiently soluble in chloroform and dichloromethane,⁴¹ were used as a surface capping agent to make ZCIS QDs possess colloidal stability and positive surface charge for potential gene delivery.⁴² QDs@PEI were fabricated by slowly injecting QDs chloroform solution into PEI water solution during ultrasonication.^{43, 44} The typical morphology of QDs@PEI was characterized by TEM. As shown in Figure 2a, QDs@PEI had a uniform diameter of ~ 40 nm, and the hydrodynamic diameter of QDs@PEI was 62.5 ± 5.4 nm, which was analyzed by the dynamic laser scattering measurements. The size increase from 7 nm (ZCIS QDs, Figure S1) to 40 nm (QDs@PEI) indicated that the hydrophobic ZCIS QDs were successfully coated with PEI due to the favorable hydrophobic interactions. The obtained QDs@PEI could be sufficiently soluble in PBS, and could emit red fluorescence under UV irradiation (Figure 2b and 2c).

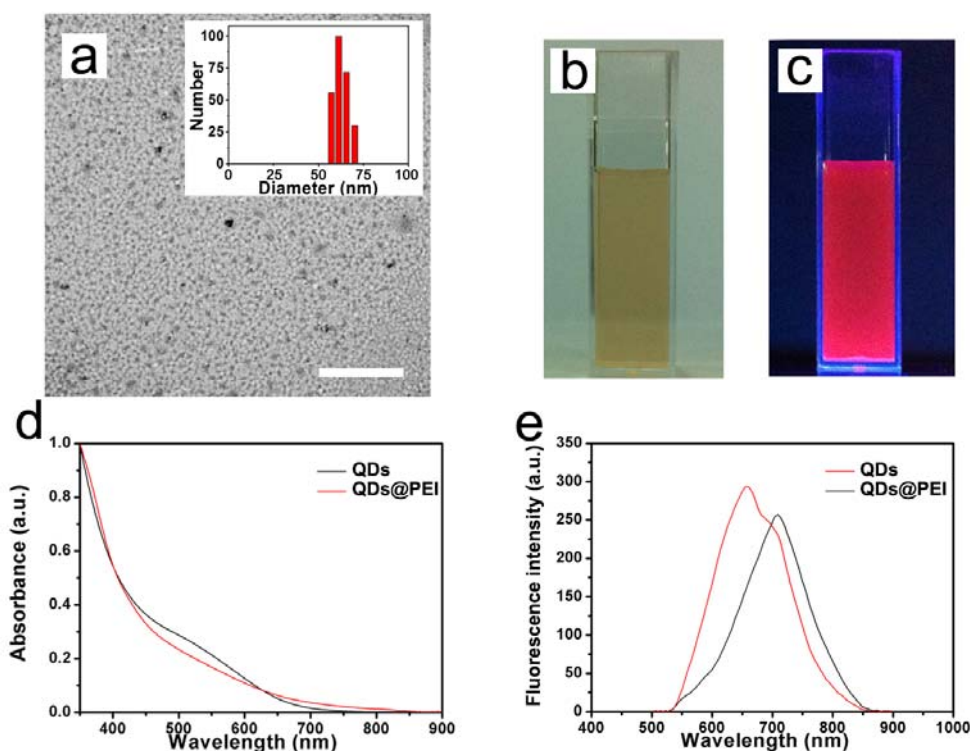


Figure 2. (a) TEM micrograph of QDs@PEI (insert: the diameter distribution of QDs@PEI), scale bar is 1 μm ; (b) and (c) photographs of QDs@PEI dispersed in PBS under sunlight and UV irradiation, respectively; UV-vis absorption (d) and fluorescence (e) spectra of QDs and QDs@PEI ($\lambda_{\text{ex}} = 350$ nm), $n=3$.

60

Cite this: DOI: 10.1039/c0xx00000x

www.rsc.org/xxxxxx

The UV-vis absorption spectra showed that QDs@PEI still had a great adsorption in the ultraviolet region after coated with PEI (Figure 2d), while the emission peak was red shift from about 655 nm to 710 nm, and the intensity decreased comparing to QDs (Figure 2e). It indicated that many single QDs aggregated to clusters (Figure 1), leading to a fluorescence quenching. The quantum yield reduced from 24 % to 20 %. The effects of pH

values (Figure S2) and ionic strengths (Figure S3) on the fluorescence of QDs@PEI was evaluated by measuring the changes of the fluorescence intensity. It was found that both pH value and ionic strengths had little effect on the fluorescence of QDs@PEI ($p > 0.05$), indicating that QDs@PEI had good stability in PBS, and could be used for *in vitro* and *in vivo* studies even at very high ionic concentration.

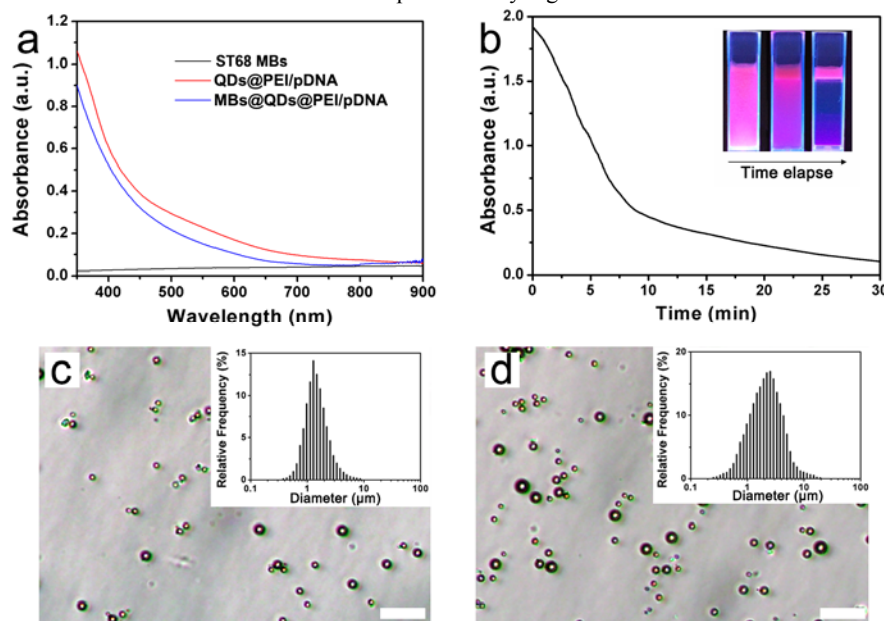


Figure 3. (a) UV-vis absorption spectra of ST68 MBs, QDs@PEI/pDNA and MBs@QDs@PEI/pDNA; (b) The absorbance changes of MBs@QDs@PEI/pDNA at 350 nm with time (inset: photographs of MBs@QDs@PEI/pDNA under UV irradiation for 0-30 min); optical microscope images of (c) ST68 MBs and (d) MBs@QDs@PEI/pDNA (inserts are size distributions for ST68 MBs and MBs@QDs@PEI/pDNA respectively), scale bar is 10 μm, $n=3$.

Gel electrophoresis analysis was used to evaluate the conjugation capability between pDNA (pEGFP-C1) and different concentrations of QDs@PEI. pDNA could be complexed with QDs@PEI through electrostatic adsorption. The QDs@PEI/pDNA complex was too large to pass through agarose gel so a retardation happened when a saturated pDNA adsorption onto QDs@PEI was achieved. Figure S4a showed that no retardation was observed with pDNA alone. Retardation began at 2.4 μM of QDs@PEI, and the degree of retardation increased with increasing the concentration of QDs@PEI. In addition, the excessive pDNA passed through agarose gel if the concentration of QDs@PEI was lower than 0.48 μM. Therefore, it was possible to see a positive zeta potential of QDs@PEI/pDNA when the concentration of QDs@PEI was above 2.4 μM, the pDNA could be firmly bound to QDs@PEI, and the mass ratio of pDNA/QDs@PEI was 1.5:1. Therefore, the QDs@PEI/pDNA complex with mass ratio of 1.5:1 was selected for the following experiment.

The zeta potential values of MBs@QDs@PEI/pDNA were measured at different assembly stages (Figure S4b). QDs@PEI had a positive potential due to the presence of amino groups of

PEI, and the potential changed from $+23.35 \pm 2.51$ mV to $+11.87 \pm 3.21$ mV after the adsorption of pDNA (5 μg) onto QDs@PEI (12 μmol). The surface potential of ST68 MBs was found to be negatively charged (-18.61 ± 3.72 mV) so the positively charged QDs@PEI/pDNA could easily adsorb onto the surface of ST68 MBs via electrostatic interaction. The potential was converted into $+4.43 \pm 1.85$ mV, indicating the successful formation of MBs@QDs@PEI/pDNA complex.

The absorption spectrum of MBs@QDs@PEI/pDNA was shown in Figure 3a in comparison with those of QDs@PEI/pDNA and ST68 MBs. The strong absorption of the QD-modified MBs in the ultraviolet region demonstrated the successful adsorption of QDs@PEI/pDNA on the surface of ST68 MBs. Figure 3b showed the dynamic reduction of the MBs@QDs@PEI/pDNA absorbance at 350 nm as time elapsed due to the delamination. MBs@QDs@PEI/pDNA came to the top of suspension after about 30 min, which was confirmed by the inset picture of Figure 3b. MBs@QDs@PEI/pDNA emitted a strong fluorescence under UV irradiation. It provided a further evidence that QDs@PEI/pDNA were successfully adsorbed onto the surface of ST68 MBs.

Optical microscope images suggested that MBs had good dispersity before and after modification with QDs@PEI/pDNA (Figure 3c and 3d). The size distributions of MBs was analyzed by static light scattering. As shown in the insets in Figure 3c and 3d, the diameters of ST68 MBs and MBs@QDs@PEI/pDNA were $1.28 \pm 0.43 \mu\text{m}$ and $2.52 \pm 2.10 \mu\text{m}$ respectively. The modification with QDs@PEI/pDNA resulted in a slight augment in the MBs diameter.⁴¹ However, more than 98 % of MBs@QDs@PEI/pDNA were less than $7 \mu\text{m}$, which could pass through pulmonary capillaries and respond to the frequencies actually used in clinical diagnostic ultrasound to produce the systemic enhancement.^{26, 27} Therefore, MBs@QDs@PEI/pDNA meet the requirement for the clinical application.

The capability for the targeted delivery of QDs@PEI/pDNA with MBs@QDs@PEI/pDNA by UTMD *in vitro* was evaluated

according to the previous report.⁴⁵ An ultrasonic transfection instrument (SonoPore KTAC-4000, NepaGene, Chiba, Japan) was used to insonate MBs@QDs@PEI/pDNA solution in PBS (pH=7.4) to simulate UTMD process *in vitro*. After insonation, the solution was filtered through $0.45 \mu\text{m}$ filters, which allowed only QDs@PEI/pDNA to pass through. Then, the concentration of zinc element from ZCIS QDs in the filtrate was measured by inductively coupled plasma optical emission spectrometry (ICP-OES). ST68 MBs were also insonated and their filtrate was used as control. The result shows that there were $45.65 \mu\text{g}$ zinc in the prepared MBs@QDs@PEI/pDNA solution, $39.31 \mu\text{g}$ zinc in the filtrate after insonation. It was calculated that about 86% of QDs@PEI/pDNA were successfully released from MBs@QDs@PEI/pDNA by UTMD.

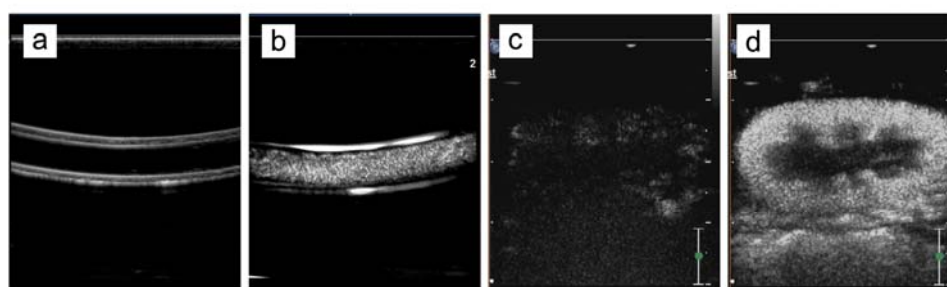


Figure 4. *In vitro* ultrasound contrast-enhanced imaging in a latex tube (a) without, (b) with MBs@QDs@PEI/pDNA; *in vivo* ultrasonograms in the rabbit right kidney: (c) before and (d) after administration of MBs@QDs@PEI/pDNA. All images are shown in PIHI (MI = 0.06) mode, n=3.

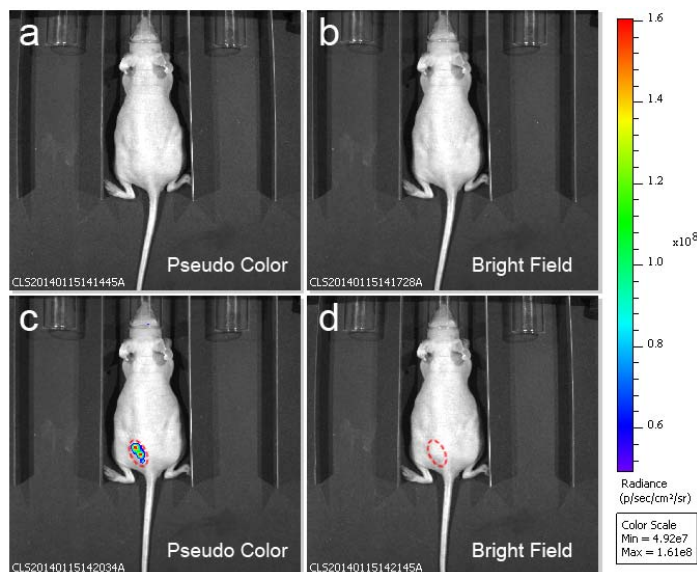


Figure 5. *In vivo* fluorescence imaging in the dorsal side of nude mouse before (a, b) and after (c, d) subcutaneously injection with MBs@QDs@PEI/pDNA, n=3.

In vitro and *In Vivo* Ultrasound Imaging

The acoustic enhancements of MBs@QDs@PEI/pDNA were evaluated both *in vitro* and *in vivo*. *In vitro* ultrasound contrast imaging was performed through injects contrast agent into a latex tube containing circulating saline.²⁸ Ultrasound contrast imaging without and with MBs@QDs@PEI/pDNA in PIHI mode as shown in Figure 4a and 4b, respectively. A significant grey scale

imaging enhancement was observed within the tube lumen in the presence of MBs@QDs@PEI/pDNA. The average grey scale of the tube lumen from ROI was increased from 24.14 ± 13.57 to 134.32 ± 48.75 ($p < 0.01$). It indicates the excellent contrast-enhancing capability of MBs@QDs@PEI/pDNA *in vitro*.

For further evaluate the *in vivo* ultrasonic response behavior of MBs@QDs@PEI/pDNA, New Zealand white rabbits were used for contrast enhanced ultrasound imaging. As shown in Figure 4c

and 4d, ultrasound imaging of rabbit kidney was greatly enhanced at PIHI mode with a mechanical index of 0.06 after injection of MBs@QDs@PEI/pDNA through the ear vein of rabbits in a few seconds. The average grey scale of the kidney from ROI was increased from 28.99 ± 21.26 to 149.51 ± 71.30 ($p < 0.01$). It proved that MBs@QDs@PEI/pDNA could operate an excellent contrast agent for ultrasound imaging. Moreover, during the entire procedure the vital signs of rabbits were normal, and no arrhythmia and other side effects were observed, thus suggesting that MBs@QDs@PEI/pDNA had no acute toxicity.

In Vivo Fluorescence Imaging

To evaluate the potential of MBs@QDs@PEI/pDNA in

fluorescence imaging, 200 μ L of MBs@QDs@PEI/pDNA were subcutaneously injected in the dorsal side of nude BALB/c mouse. The fluorescence images were obtained at 430 nm excitation and captured at 700 nm. As shown in Figure 5, no fluorescence signal was detected before the injection (Figure 5a and 5b). However, a obviously fluorescence signal was observed in the dorsal side injected with MBs@QDs@PEI/pDNA (Figure 5c and 5d). The intensity of region of interest (ROI) was increased to $(1.86 \pm 0.26) \times 10^{11}$ ($p < 0.01$). It showed that the emission of MBs@QDs@PEI/pDNA at 700 nm had a good tissue penetration depth which could be used for NIR fluorescence imaging *in vivo*.

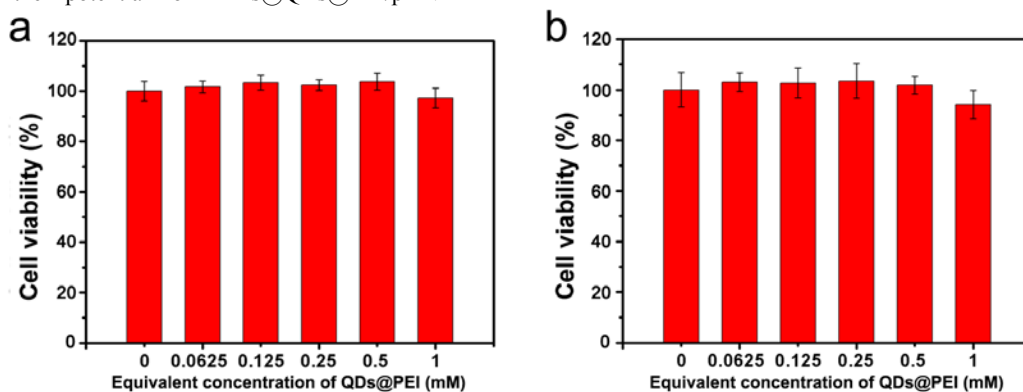


Figure 6. viabilities of HUVEC cells (a) and HeLa cells (b) after incubation with different concentrations of MBs@QDs@PEI/pDNA for 48 h. Data shown as mean standard deviation (SD), n=5.

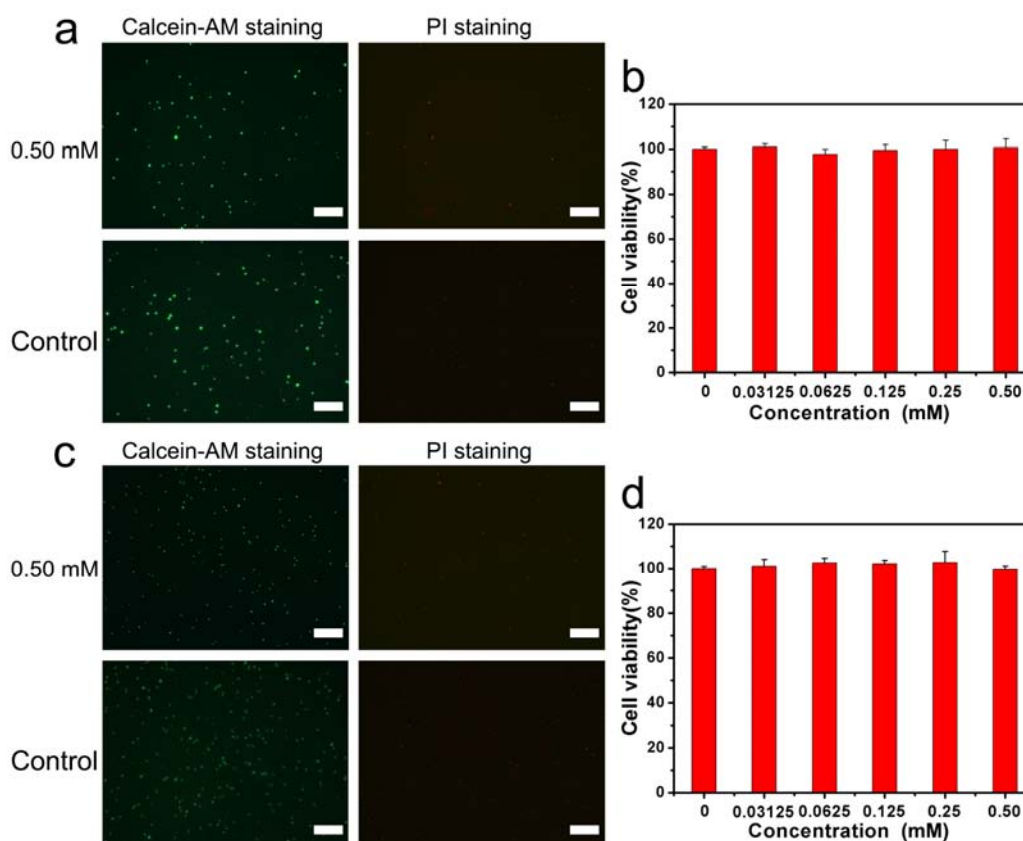


Figure 7. Fluorescence microscopy images of BMDCs cell (a) and T cell (c) after treatment with different concentration of MBs@QDs@PEI/pDNA stained with calcein AM and PI; The cell survival rate of BMDCs cell (b) and T cell (d) after treatment with different concentration of MBs@QDs@PEI/pDNA for 24h. Scale bar is 500 μ m. Data shown as mean SD, n=5.

Biocompatibility Evaluation

After confirming the feasibility of ultrasonic/NIR fluorescence bi-modal imaging using MBs@QDs@PEI/pDNA, the biocompatibility of MBs@QDs@PEI/pDNA was also evaluated. Both Human umbilical vein endothelial (HUVEC) cells and HeLa cells were incubated with different concentrations of MBs@QDs@PEI/pDNA for 48 h. Then, the viability of HUVEC cells and HeLa cells were tested by MTT method. As shown in Figure 6, the cell viabilities of HUVEC cells and HeLa cells were still above 90% at the concentration as high as 1 mM ($p > 0.05$). It

indicated that MBs@QDs@PEI/pDNA were highly biocompatible both in healthy cells and tumor cells. The cytotoxicity of PEI/pDNA and QDs@PEI/pDNA to HeLa cells were also tested by MTT method. As shown in Figure S5, QDs@PEI/pDNA exhibited a notably higher half maximal inhibitory concentration (IC_{50}) than PEI/pDNA (158.37 mg L^{-1} versus 6.84 mg L^{-1}) after incubated with HeLa cells for 48h ($p < 0.01$). It indicated that the QDs@PEI/pDNA has a better biocompatible than PEI/pDNA.

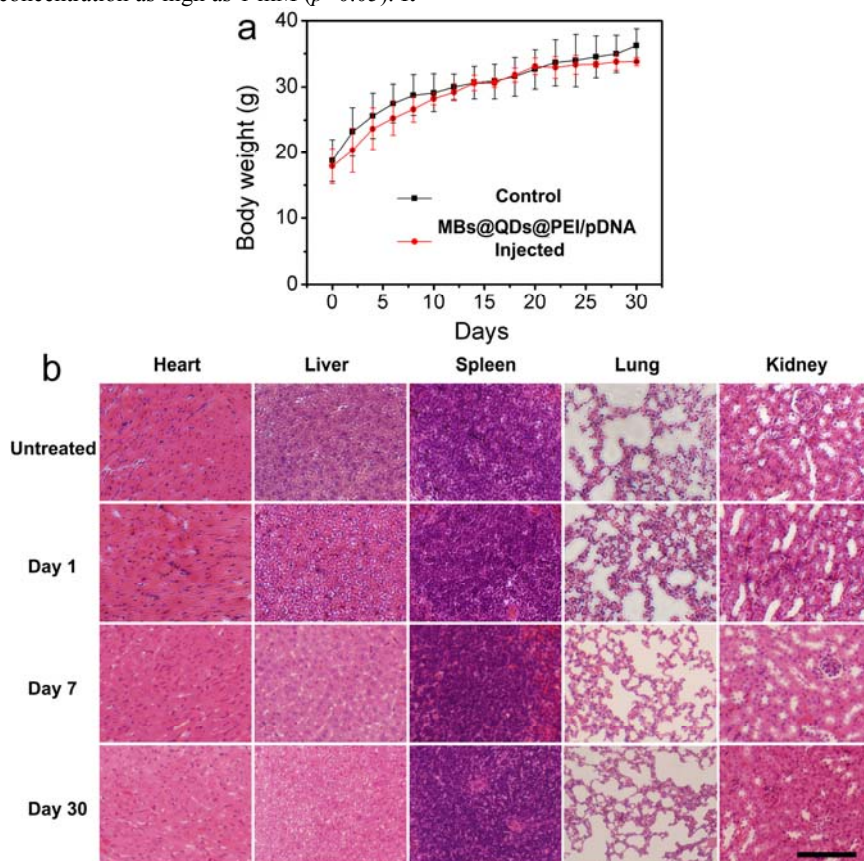


Figure 8. (a) Body weight curves after intravenous administration of MBs@QDs@PEI/pDNA; (b) Histological section of vital organs (heart, liver, spleen, lung and kidneys) stained with hematoxylin and eosin at day 1, day 7 and day 30 after intravenous administration of MBs@QDs@PEI/pDNA, the untreated group was used as the control. Scale bar is 100 μm . Data shown as mean SD, $n=5$.

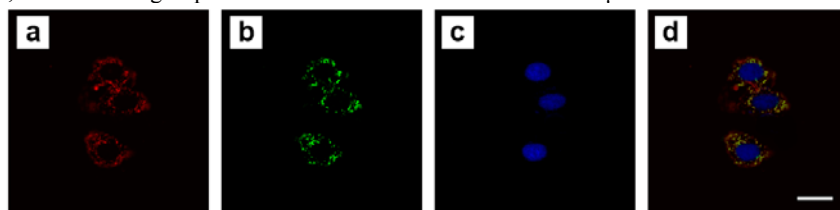


Figure 9. Subcellular localization of QDs@PEI/pDNA in HeLa cells observed by CLSM: (a) QDs@PEI/pDNA channel; (b) LysoTracker Green channel; (c) DAPI channel; (d) overlap of (a), (b) and (c). Scale bar is 20 μm , $n=3$.

To further determine the biocompatibility of MBs@QDs@PEI/pDNA, Bone marrow dendritic cells (BMDC) and T cell were incubated with MBs@QDs@PEI/pDNA for 24 h. And then viable cells and dead cells were stained as green fluorescence from calcein acetoxyethyl ester (calcein-AM) and red fluorescence from propidium iodide (PI) respectively.

Fluorescence microscopy images indicated no significant effect observed both on BMDC and T cell after treatment with 0.5 mM MBs@QDs@PEI/pDNA (Figure 7a and 7c). For qualitative analysis, cell viabilities were also examined by MTT assay. As shown in Figure 7b and 7d, MBs@QDs@PEI/pDNA had little effect on cell viability ($p > 0.05$). All these results verified that

MBs@QDs@PEI/pDNA had good biocompatibility and could be used for *in vivo* research.

For further evaluate the *in vivo* toxicity of MBs@QDs@PEI/pDNA in mice, MBs@QDs@PEI/pDNA (300 μ M, 200 μ L) were intravenously administered into mice. After 30 days post-injection, neither death nor significant body weight loss was noticed ($p > 0.05$) (Figure 8a). Histological sections of major organs (heart, liver, spleen, lung and kidneys) were stained with hematoxylin and eosin (H&E). No apparent lesion in cellular structures was observed at day 1, day 7 and day 30 after intravenous administration of MBs@QDs@PEI/pDNA (Figure 8b). It proved a further evidence that MBs@QDs@PEI/pDNA had no obvious toxicity to mice.

Cellular Uptake of QDs@PEI/pDNA

HeLa cells were incubated with the QDs@PEI/pDNA dispersion and the uptake of QDs@PEI/pDNA was observed via confocal laser scanning microscopy (CLSM). In Figure 9a, a red fluorescence showed clearly that QDs@PEI/pDNA complexes were distributed in the cytoplasm after incubation for 24 h. The lysosome was stained into green fluorescence by LysoTracker Green DND (Figure 9b). The blue fluorescence in Figure 9c was the cell nuclei of HeLa cells which stained with 4',6-diamidino-2-phenylindole (DAPI). It suggested that QDs@PEI/pDNA complexes could be easily internalized by HeLa cells through endocytosis.

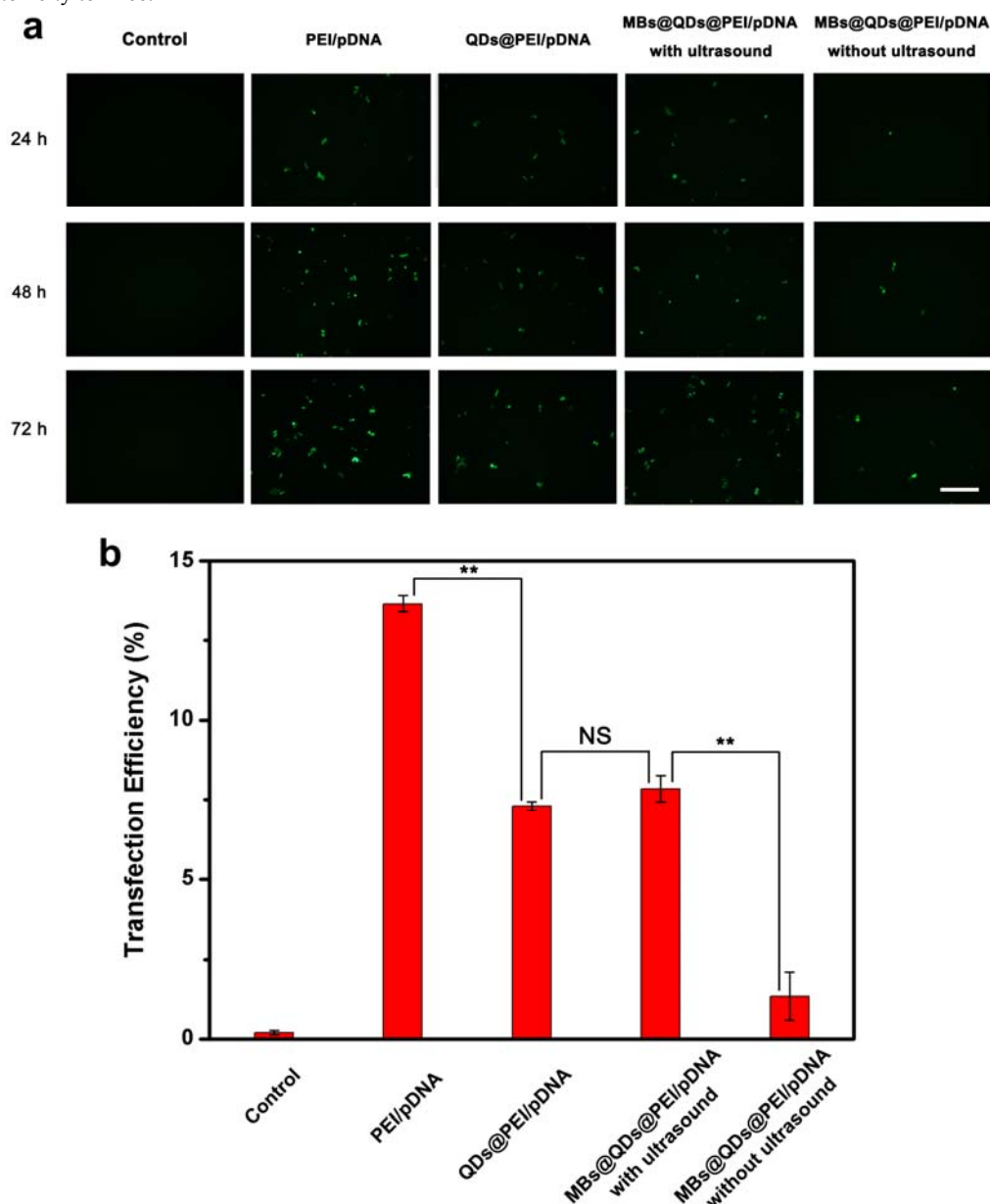


Figure 10. (a) Fluorescence microscope images of pEGFP-C1 transfected HeLa cells treated with PEI, QDs-PEI, MBs@QDs@PEI with and without ultrasound irradiation for 24 h, 48 h and 72 h; (b) transfection efficiency of PEI, QDs@PEI, MBs@QDs@PEI with and without ultrasound irradiation toward HeLa cells by flow cytometry. Scale bar is 200 μ m. Data shown as mean SD, $n=5$. Significance was defined as $p < 0.05$ (NS, non-significance, $*p < 0.05$, $**p < 0.01$).

Cite this: DOI: 10.1039/c0xx00000x

www.rsc.org/xxxxxx

Transfection Experiment

To evaluate the potential application of MBs@QDs@PEI for pDNA (pEGFP-C1) delivery, *in vitro* transfection experiments were conducted with HeLa cells in comparison with pDNA (set as control), PEI/pDNA, QDs@PEI/pDNA, MBs@QDs@PEI/pDNA with and without ultrasound irradiation. The expression of green fluorescent protein (GFP) was observed under inverted fluorescence microscope. It was found that the transfection efficiency increased with the incubation time from 24 h to 72 h (Figure 10a). On the other hand, the transfection efficiency of QDs@PEI was lower than PEI. An ultrasound transfection instrument has used to evaluate the transfection efficiency of MBs@QDs@PEI under ultrasound irradiation. There was a slight improvement compared with QDs@PEI at the same equivalent concentration of QDs@PEI. However, transfection efficiency of MBs@QDs@PEI without ultrasound was very low. By flow cytometry analysis, the pEGFP-C1 transfection efficiencies of PEI, QDs@PEI and MBs@QDs@PEI after 72 h incubation were further quantified to be $13.65\pm 0.27\%$ for PEI, $7.30\pm 0.14\%$ for QDs@PEI, $7.85\pm 0.43\%$ and $1.35\pm 0.76\%$ for MBs@QDs@PEI with and without ultrasound irradiation, respectively (Figure 10b). As expected, the transfection efficiency of QDs@PEI and MBs@QDs@PEI were lower than PEI ($p < 0.01$). But, it is a relative high transfection efficiency of MBs@QDs@PEI than QDs@PEI ($p > 0.05$). Moreover, the transfection efficiency of MBs@QDs@PEI with ultrasound irradiation was significant higher than that of without ultrasound irradiation ($p < 0.01$). This phenomenon might be caused by the cavitation effect generated from ultrasound irradiation during the UTMD operation. Furthermore, in the MBs@QDs@PEI without ultrasound irradiation, pDNA could not internalize into cells since it was floating on the medium with MBs@QDs@PEI. Escoffre et al. evaluated the transfection ability of Vevo Micromarker microbubbles induced by UTMD, the transfection efficiency could reach to 70%.³⁰ However, the Vevo Micromarker microbubbles can not monitor the gene delivery due to the absence of intrinsic fluorescence. Attributed to the conjugation of NIR QDs, the pDNA delivery could be tracked by NIR fluorescence imaging. Therefore, MBs@QDs@PEI take an advantage for the image-guided gene therapy.

Conclusions

In summary, a multifunctional ultrasound contrast agent was successfully fabricated by adsorption of pDNA complexed ZCIS QDs onto the surface of ST68 MBs. Both *in vitro* and *in vivo* results showed that the obtained composite agent of MBs@QDs@PEI/pDNA had excellent capability to enhance both ultrasound and fluorescence imaging. Through UTMD, the "soft" ST68 MBs could release QDs@PEI/pDNA into target tissue to achieve efficient gene therapy, which could be noninvasively and quantitatively monitored in real time by NIR fluorescence/ultrasound biomodal imaging. In addition, such a multifunctional

agent could operate as a general platform for the NIR fluorescent/ultrasonic bimodal imaging guided therapy by loading the other therapeutic agents (doxorubicin, paclitaxel, siRNA etc.) and medical nanoparticles (gold, graphene oxide and Fe₃O₄ etc.). This would enable personalized detection and treatment of diseases with high efficacy.

Acknowledgments

This work was financially supported by National Natural Science Foundation of China (No. 81371580 and 81171347) and State Key Program of National Natural Science of China (No. 81230036).

Notes and references

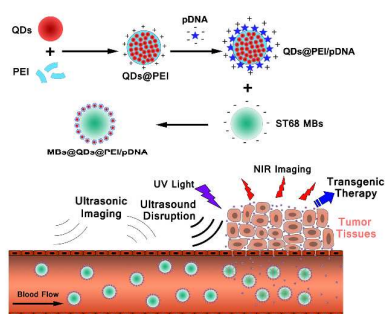
^a School of Municipal and Environmental Engineering and School of Life Science and Technology, Harbin Institute of Technology, Harbin 150001, China. Email: xiulidx@163.com

^b Department of Ultrasonography, Peking University Third Hospital, Beijing 100083, China.

Electronic Supplementary Information (ESI) available: [Additional TEM micrograph of ZCIS QDs, Effects of pH values and ionic strengths on the fluorescence of QDs@PEI, Agarose gel electrophoresis analysis, zeta potential analysis and cell viabilities QDs@PEI/pDNA and PEI/pDNA]. See DOI: 10.1039/b000000x/

1. W. F. Anderson, *Nature*, 1998, **392**, 25.
2. P. R. Dash, M. L. Read, L. B. Barrett, M. A. Wolfert and L. W. Seymour, *Gene Ther*, 1999, **6**, 643.
3. C. X. Li, A. Parker, E. Menocal, S. Xiang, L. Borodyansky and J. H. Fruehauf, *Cell Cycle*, 2006, **5**, 2103.
4. Y. Song, H. Wang, X. Zeng, Y. Sun, X. Zhang, J. Zhou and L. Zhang, *Bioconjug Chem*, 2010, **21**, 1271.
5. P. P. Karmali and A. Chaudhuri, *Med Res Rev*, 2007, **27**, 696.
6. Y. Liang, Z. Liu, X. Shuai, W. Wang, J. Liu, W. Bi, C. Wang, X. Jing, Y. Liu and E. Tao, *Biochem. Biophys. Res. Commun.*, 2012, **421**, 690.
7. H. Wei, L. R. Volpatti, D. L. Sellers, D. O. Maris, I. W. Andrews, A. S. Hemphill, L. W. Chan, D. S. Chu, P. J. Horner and S. H. Pun, *Angew Chem Int Ed Engl*, 2013, **52**, 5377.
8. S. R. Sirsi and M. A. Borden, *Theranostics*, 2012, **2**, 1208.
9. J. Y. Yhee, S. J. Lee, S. Lee, S. Song, H. S. Min, S. W. Kang, S. Son, S. Y. Jeong, I. C. Kwon, S. H. Kim and K. Kim, *Bioconjug Chem*, 2013, **24**, 1850.
10. Y. Zhang and T. H. Wang, *Theranostics*, 2012, **2**, 631.
11. J. M. Li, M. X. Zhao, H. Su, Y. Y. Wang, C. P. Tan, L. N. Ji and Z. W. Mao, *Biomaterials*, 2011, **32**, 7978.
12. B. Dubertret, P. Skourides, D. J. Norris, V. Noireaux, A. H. Brivanlou and A. Libchaber, *Science*, 2002, **298**, 1759.
13. X. Wu, H. Liu, J. Liu, K. N. Haley, J. A. Treadway, J. P. Larson, N. Ge, F. Peale and M. P. Bruchez, *Nat. Biotechnol.*, 2003, **21**, 41.

14. X. Gao, Y. Cui, R. M. Levenson, L. W. Chung and S. Nie, *Nat. Biotechnol.*, 2004, **22**, 969.
15. D. R. Larson, W. R. Zipfel, R. M. Williams, S. W. Clark, M. P. Bruchez, F. W. Wise and W. W. Webb, *Science*, 2003, **300**, 1434.
16. R. S. Burke and S. H. Pun, *Bioconjug Chem*, 2008, **19**, 693.
17. W. Zhang and X. Zhong, *Inorg. Chem.*, 2011, **50**, 4065.
18. J. Feng, M. Sun, F. Yang and X. Yang, *Chem Commun (Camb)*, 2011, **47**, 6422.
19. H. Yang, H. Mao, Z. Wan, A. Zhu, M. Guo, Y. Li, X. Li, J. Wan, X. Yang, X. Shuai and H. Chen, *Biomaterials*, 2013, **34**, 9124.
20. Z. Dai, B. Peng and X. Chen, *Dyes Pigm.*, 1999, **40**, 219-223.
21. Z. Dai, A. Voigt, E. Donath and H. Möhwald, *Macromol. Rapid Commun.*, 2001, **22**, 756-762.
22. X. Yang, Z. Dai, A. Miura and N. Tamai, *Chem. Phys. Lett.*, 2001, **334**, 257-264.
23. L. D. Chen, J. Liu, X. F. Yu, M. He, X. F. Pei, Z. Y. Tang, Q. Q. Wang, D. W. Pang and Y. Li, *Biomaterials*, 2008, **29**, 4170.
24. A. M. Smith, H. Duan, A. M. Mohs and S. Nie, *Adv Drug Deliv Rev*, 2008, **60**, 1226.
25. D. Deng, J. Xia, J. Cao, L. Qu, J. Tian, Z. Qian, Y. Gu and Z. Gu, *J. Colloid Interface Sci.*, 2012, **367**, 234.
26. H. Ke, J. Wang, Z. Dai, Y. Jin, E. Qu, Z. Xing, C. Guo, X. Yue and J. Liu, *Angew Chem Int Ed Engl*, 2011, **50**, 3017.
27. H. Ke, J. Wang, Z. Dai, Y. Jin, E. Qu, Z. Xing, C. Guo, J. Liu and X. Yue, *J. Mater. Chem.*, 2011, **21**, 5561.
28. H. Ke, Z. Xing, B. Zhao, J. Wang, J. Liu, C. Guo, X. Yue, S. Liu, Z. Tang and Z. Dai, *Nanotechnology*, 2009, **20**, 425105.
29. R. V. Shohet, S. Chen, Y. T. Zhou, Z. Wang, R. S. Meidell, R. H. Unger and P. A. Grayburn, *Circulation*, 2000, **101**, 2554.
30. J. M. Escoffre, A. Novell, J. Piron, A. Zeghimi, A. Doinikov and A. Bouakaz, *IEEE Trans. Ultrason. Ferroelectr. Freq. Control*, 2013, **60**, 46-52.
31. J. M. Escoffre, A. Zeghimi, A. Novell, and A. Bouakaz, *Curr Gene Ther*, 2013, **13**, 2-14.
32. B. F. Yu, J. Wu, Y. Zhang, H. W. Sung, J. Xie and R. K. Li, *Cancer Gene Ther*, 2013, **20**, 290.
33. D. Yang, Y. H. Gao, K. B. Tan, Z. X. Zuo, W. X. Yang, X. Hua, P. J. Li, Y. Zhang and G. Wang, *Gene Ther*, 2013, **20**, 1140.
34. I. Lentacker, B. G. De Geest, R. E. Vandenbroucke, L. Peeters, J. Demeester, S. C. De Smedt and N. N. Sanders, *Langmuir*, 2006, **22**, 7273-7278.
35. J. M. Escoffre, C. Mannaris, B. Geers, A. Novell, I. Lentacker, M. Averkiou and A. Bouakaz, *IEEE Trans. Ultrason. Ferroelectr. Freq. Control*, 2013, **60**, 78-87.
36. M. Ward, J. Wu and J. F. Chiu, *Ultrasound Med Biol*, 2000, **26**, 1169.
37. R. J. Price, D. M. Skyba, S. Kaul and T. C. Skalak, *Circulation*, 1998, **98**, 1264.
38. Z. Dai, J. T. Wilson and E. L. Chaikof, *Materials Science & Engineering C-Biomimetic and Supramolecular Systems*, 2007, **27**, 402-408.
39. L. Li, T. J. Daou, I. Texier, T. T. Kim Chi, N. Q. Liem and P. Reiss, *Chem. Mater.*, 2009, **21**, 2422.
40. R. Basude, J. W. Duckworth and M. A. Wheatley, *Ultrasound Med Biol*, 2000, **26**, 621.
41. T. Nann, *Chem Commun (Camb)*, 2005, 1735.
42. G. Liu, Z. Wang, S. Lee, H. Ai and X. Chen, *Methods Enzymol.*, 2012, **509**, 263.
43. A. Romoser, D. Ritter, R. Majitha, K. E. Meissner, M. McShane and C. M. Sayes, *PLoS One*, 2011, **6**, e22079.
44. H. N. Yang, J. S. Park, D. G. Woo, S. Y. Jeon and K. H. Park, *Biomaterials*, 2012, **33**, 8670.
45. Z. Zha, S. Wang, S. Zhang, E. Qu, H. Ke, J. Wang and Z. Dai, *Nanoscale*, 2013, **5**, 3216-3219.



MBs@QDs@PEI/pDNA was prepared to operate as a NIR/Ultrasound bimodal imaging guided platform for targeting deliver pDNA by UTMD.